



Article

Enable High-Energy $\text{LiNi}_{0.5}\text{Co}_{0.2}\text{Mn}_{0.3}\text{O}_2$ by Ultra-Thin Coating through Wet Impregnation

Xin Su ^{1,2}, Xiaoping Wang ¹, Javier Barenco ¹, Yan Qin ¹, Frederic Aguesse ¹ and Wenquan Lu ^{1,*}¹ Chemical Sciences and Engineering Division, Argonne National Laboratory, 9700 South Cass Avenue, Lemont, IL 60439-4837, USA² School of New Energy, Harbin Institute of Technology, Weihai, 2 West Wenhua Road, Weihai 264209, China

* Correspondence: luw@anl.gov; Tel.: +1-(630)-252-3704; Fax: +1-(630)-252-4176

Abstract: A high cut-off voltage is required for nickel-rich layered oxide $\text{LiNi}_x\text{Co}_y\text{Mn}_z\text{O}_2$ (NCM) to meet the high energy density requirement of lithium-ion batteries in electric vehicles. However, such a high voltage application leads to an unstable interface between NCM and liquid electrolytes. To stabilize the interface, the facile wet impregnation method has been developed to apply an ultra-thin Al_2O_3 coating layer on the NCM particles. This coating layer was found to have a strong interaction with the NCM and resulted in Al-doped NCM at the surface structure of NCM. The change of surface structure can not only reduce the surface resistance of lithium diffusion of $\text{LiNi}_{0.5}\text{Co}_{0.2}\text{Mn}_{0.3}\text{O}_2$ (NCM523), but also stabilize the solid electrolyte interface between NCM523 and the electrolyte with the cut-off voltage of 4.5 V vs. Li/Li⁺. Compared to other coating methods, wet impregnation coating can provide an ultra-thin and uniform coating with surface doping on NCM particles. Furthermore, this scalable coating method can be applied to various electrode materials without adding much additional cost.



Citation: Su, X.; Wang, X.; Barenco, J.; Qin, Y.; Aguesse, F.; Lu, W. Enable High-Energy $\text{LiNi}_{0.5}\text{Co}_{0.2}\text{Mn}_{0.3}\text{O}_2$ by Ultra-Thin Coating through Wet Impregnation. *Batteries* **2022**, *8*, 136. <https://doi.org/10.3390/batteries8100136>

Academic Editor: Carlos Zieber

Received: 2 August 2022

Accepted: 19 September 2022

Published: 21 September 2022

Publisher's Note: MDPI stays neutral with regard to jurisdictional claims in published maps and institutional affiliations.



Copyright: © 2022 by the authors. Licensee MDPI, Basel, Switzerland. This article is an open access article distributed under the terms and conditions of the Creative Commons Attribution (CC BY) license (<https://creativecommons.org/licenses/by/4.0/>).

1. Introduction

The nickel-rich layered oxides $\text{LiNi}_x\text{Co}_y\text{Mn}_z\text{O}_2$ (NCM) are promising cathode materials for lithium-ion batteries (LIBs) due to their high energy density, low cost, and low toxicity [1–6]. In NCM, a redox reaction centered around Ni²⁺ and Co³⁺ accounts for the capacity of the cathode, while the inactive Mn⁴⁺ is helpful in stabilizing the structure during charging/discharging [7–10]. Among all NCM materials, $\text{LiNi}_{0.5}\text{Co}_{0.2}\text{Mn}_{0.3}\text{O}_2$ (NCM523) has attracted extensive research effort, since the ratio among nickel, cobalt, and manganese allows it to balance the demand for high capacity and structural stability [3,10,11].

Recently, the demands from the electric vehicle (EV) industry regarding the energy density and cycle life of lithium-ion batteries have dramatically increased. A high cut-off voltage is required for NCM to meet the high energy density requirement of LIBs in EVs. However, a high voltage application leads to an unstable interface between NCM and the liquid electrolyte. Coating the cathode has been widely investigated to improve interfacial stability due to the following benefits: the coating may slow down transition metal dissolution by reducing the direct contact between the cathode and the electrolyte; the coating may also serve as an HF scavenger, locally reducing electrolyte decomposition.

Al_2O_3 has been widely adopted as a coating for cathode materials due to its excellent electrochemical, chemical, and thermal stability [12–15]. It can also work as an excellent protective layer for cathode materials. Various coating approaches have been developed including (1) chemical vapor deposition [16–18], (2) atomic layer deposition [13–15], (3) radio frequency magnetron sputtering [19], (4) organic pyrolysis [12], (5) co-precipitation [20], (6) the sol-gel method [21], (7) electroless plating [22], and (8) the solvothermal technique [23]. In general, the gas-based approaches can offer a uniform coating but are

not cost-efficient, which usually implies the need for expensive equipment with low efficiency [24–29]. Meanwhile, the liquid-based techniques are cost-efficient but it is difficult to obtain good quality coating. [12,20–23] Therefore, the cost-efficient approach with a high-quality coating is highly demanded by NCM.

Presented here is a facile approach for coating an ultra-thin Al_2O_3 layer on NCM523. It is a simple coating process, which not only improves the cycle life of NCM523 with the cut-off voltage of 4.5 V vs. Li/Li⁺, but also surprisingly increases the specific capacity. A detailed analysis suggested that the coated Al_2O_3 had a strong interaction with NCM523 and that the surface layer of NCM523 was doped by Al. Therefore, the ultra-thin Al_2O_3 coating by wet impregnation can not only improve the surface stability of NCM523 during a cycle test, but also reduce the surface resistance.

2. Experimental Section

2.1. Surface Modification Process of NCM523

The surface modification of the NMC523 cathode powder was realized by generating a thin layer of Al_2O_3 coating on the cathode powder surface via the wet impregnation method, as shown in Figure 1. In this method, the desired amount of an aluminum salt precursor was dissolved in a small volume of deionized water, forming a solution. The solution was then thoroughly mixed with the cathode powder, followed by an overnight drying step at 120 °C. Finally, the mixture was calcined at 450 °C for four hours, during which decomposition of the salt occurred, leading to a thin Al_2O_3 coating layer.

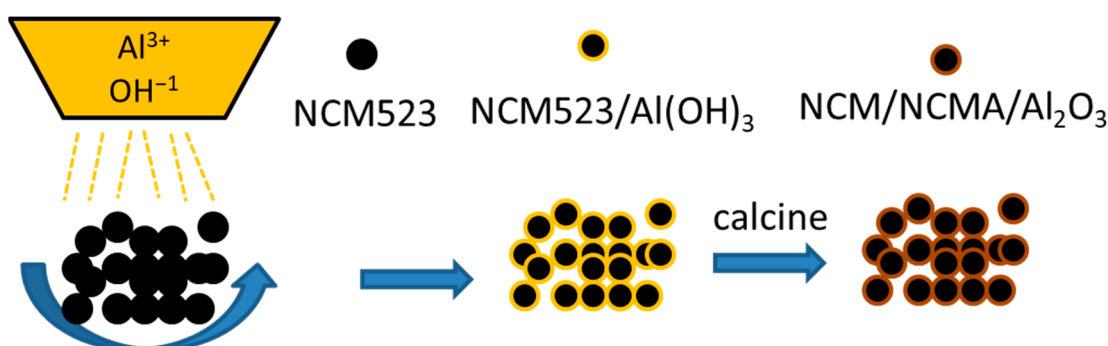


Figure 1. Schematic picture of the facile process for surface coating doping NCM523.

2.2. Characterization of Pristine and Surface-Modified NCM523

The surface of the pristine and modified NCM523 powders were characterized using a scanning electron microscope (SEM, Hitachi S-4700 at 10 kV) equipped with energy dispersive spectroscopy (EDS). Additionally, the surface elements and their chemical status for the NCM523 powder with/without modification were further characterized by X-ray photoelectron spectroscopy (XPS). The XPS data were collected using a scanning XPS microprobe. The background pressure in the XPS was between 6×10^{-10} and 3×10^{-9} Torr, while the pressure during work was about 2×10^{-8} Torr. XPS spectra were obtained in a fixed analyzer mode with the X-ray beam of the 100 mm diameter from the Al Ka source (1486.7 eV). The source output offered a power of 60 W with the emission current of 4 mA and an acceleration voltage of 15 kV. The different elemental regions were recorded using a pass energy of 23.5 eV and a step size of 0.2 eV. Meanwhile, the number of scans and dwell time were adjusted to optimize the signal-to-noise ratio. All scans were averaged and normalized by the dwell time. Further peak position correction was carried out by referencing the C 1s peak position. With this native resolution set, peaks were added.

2.3. The Preparation of the Cathode Using Pristine and Modified NCM523 and the Corresponding Anode

The preparation of the cathodes using pristine and NCM523 with surface modification was carried out as follows: slurry making, casting, drying, and calendering. The pris-

tine/modified NCM523 and carbon black (Timcal C45, 5 wt.%) were mixed with a solution of polyvinylidene difluoride (PVDF, Solvay 5310) in N-methyl-2-pyrrolidone. The slurry was mixed using a Thinky mixer ARE-310 and then coated onto an aluminum (Al) foil. The coating was dried at 75 °C for 4 h and further dried at 75 °C in a vacuum for 12 h to the electrode. The electrode was then calendered to the target thickness. The electrodes were finally dried at 120 °C in a vacuum for >4 h before being assembled into the coin cells (2032). The final composition of the electrodes was 90% NCM523, 5% PVDF, and 5% carbon black. The electrode coating on the Al foil was kept at ~8.7 mg/cm² and 30% porosity. Electrode area was 1.54 cm². Lithium metal was used as a counter electrode for half-cells. For the full cell, the formulation of the corresponding anode was 91.8% graphite, 2% carbon black (Timcal Super C45), 6% PVDF (Kureha 9300), and 0.17% oxalic acid, which was provided by Argonne National Laboratory's Cell Analysis Modeling Prototyping (CAMP) Facility. The loading of anodes on copper was ~5.9 mg/cm², with 38% porosity. The electrode area of the anode was 1.77 cm². The electrolyte of 1.2 M LiPF₆ in ethylene carbonate (EC)/ethyl methyl carbonate (EMC) (30/70 by weight) was used in the cells.

2.4. Electrochemical Measurements of the Half and Full Cells Using Pristine and Modified NCM523

Galvanostatic cycling tests of the half and full cells using pristine and modified NCM523 were conducted using a MacCor series 4000 potentiostat at room temperature. The initial three formation cycles of the half-cells were carried out between 3.0 V and 4.5 V vs. Li/Li⁺ at 0.1 C and the room temperature to obtain the capacities and voltage profiles. Then, the half-cells were tested at rates from C/5, C/3, C/2, 1C, to 2C and between 3.0 V and 4.5 V. Finally, the cycling tests of the half-cells were carried out at C/3 and room temperature.

Hybrid pulse power characterization (HPPC) was conducted during the cycling test. During the HPPC, a 2 C discharge pulse (10 s) and a 1.5 C regenerative charge pulse were applied to the half-cell with 40 s rest periods between discharge and regenerative pulses. The test profile was conducted each 10% depth of discharge (DOD). The area-specific impedance (ASI), as a function of the DOD, was obtained by calculating the voltage changes during the pulses. The test procedures for the full cell were the same as those for the half-cell except for a voltage range change from 3.0–4.5 V to 3.0–4.4 V to accommodate the potential difference between the lithium and graphite anodes in the cells.

3. Result and Discussion

The surface modification of NCM523 was achieved by impregnating the aqueous aluminum salt solution on the NCM523 surface, targeting 0.1% Al₂O₃. Based on the loading amount and calculation, the average thickness of the coating on NCM523 particles was ~3 nm. This has been confirmed by XPS results later, which is a surface analytical tool with about 5 nm of detection depth. As shown in low and high magnification, SEM images of the pristine NCM523 (Figure 2a,b, respectively) and the modified NCM523 (Figure 2c,d, respectively), the surface morphologies of the NCM523 particles before and after the surface modification process remained the same. Meanwhile, the EDS on the surface-modified NCM523 particles showed that elemental Al was on them. This indicates that the ultra-thin coating on NCM523 had been successfully created without any agglomeration.

To obtain more detailed information about the coating, XPS was carried out for the pristine and surface-modified NCM523 samples. XPS spectra of transition metals Ni, Co, and Al are shown in Figure 3a. The same XPS peaks are observed for Ni 3s and Co 3s in both the pristine and modified NCM523, while Al 2s for the Al element is detected on the modified NCM523. These results suggest that the Al was coated on the surface of NCM523, which was very thin and did not mask Ni and Co. A broad O 1s XPS peak around 532.1 eV is observed for pristine NCM523 in Figure 3b. However, two O 1s peaks at lower binding energies, 527.5 eV and 529.5 eV, are observed for surface-modified NCM523. The O 1s peak at 527.5 eV was assigned to oxygen from the Al₂O₃ [30]. Meanwhile, the O 1s peak for oxygen in NCM523 shifted from 532.1 eV to 529.5 eV, which indicates that there was a new

O environment, suggesting that Al may not only exist as Al_2O_3 but that it also gets into the lattice structure of NCM523 [30].

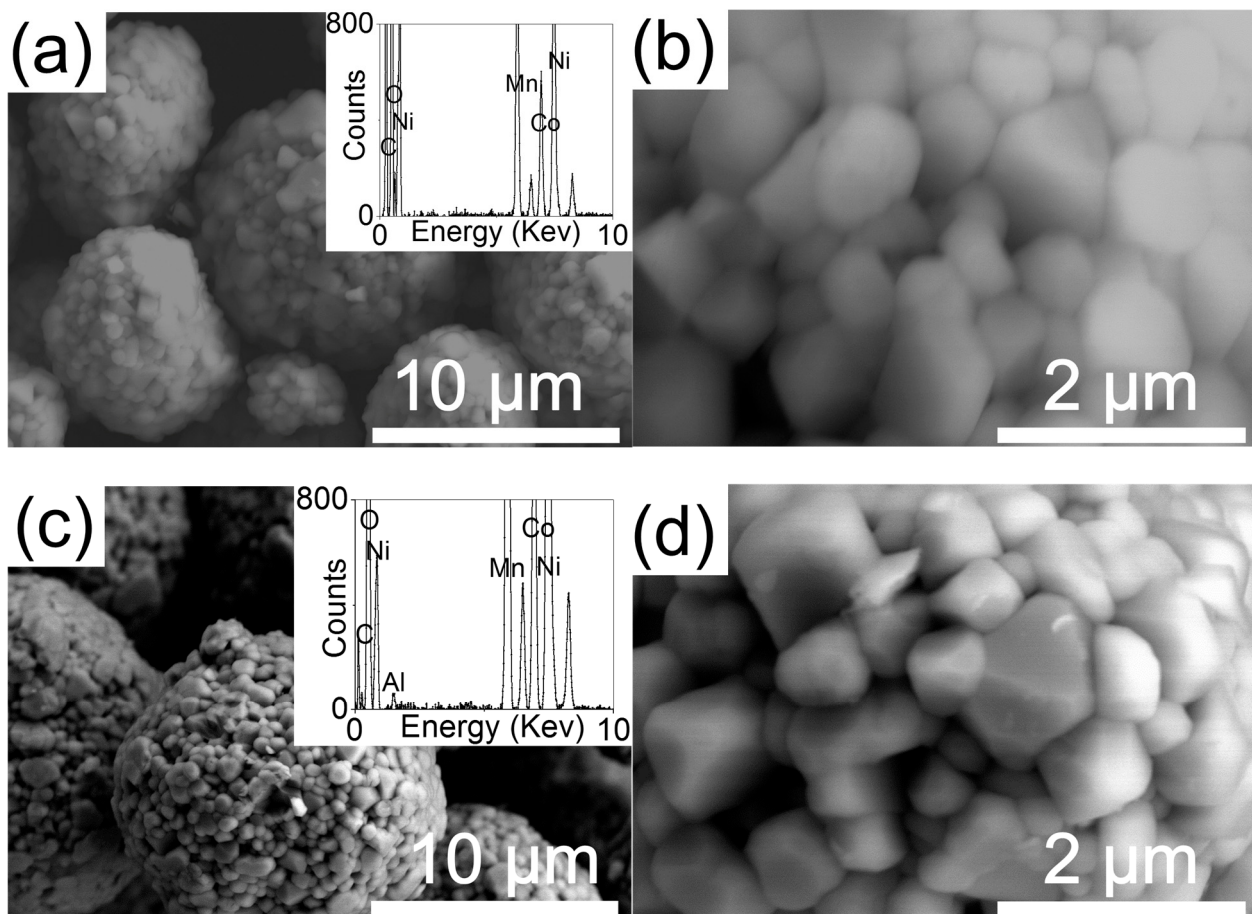


Figure 2. High and low magnification SEM/EDS of (a,b) pristine NCM523 and (c,d) NCM523 with Al_2O_3 coating doping.

Furthermore, compared to the peaks for Mn 2p at ~643 eV, Co 2p at ~781 eV, and Ni 2p at ~856 eV of pristine NCM523, those of the modified NCM523 are broader and expanded to the lower binding energy, as shown in Figure 3c–e. These results indicate that besides the existing peaks, there are new peaks for Mn 2p at ~640 eV, Co 2p at ~778 eV, and Ni 2p ~853 eV. The binding energy shifts of Ni, Co, and Mn also suggest the environment change of NCM523. We believe that wet impregnation is capable of forming an ultra-thin Al_2O_3 precursor coating on NCM523. During calcination, the precursors not only transform into an Al_2O_3 coating layer but also diffuse into the NCM523 lattice structure and become Al-doped NCM523 (NCMA) [31,32]. Therefore, our coating method creates an ultra-thin surface layer of $\text{Al}_2\text{O}_3/\text{NCMA}$ on NCM523 rather than just an Al_2O_3 layer.

The surface-modified NCM523 by this approach increases its specific capacity in the half-cell from 192 to 201 mAh/g with the cut-off voltage of 4.5 V vs. Li/Li⁺ in Li/NCM523 half-cells, as shown in Figure 4a. As far as we know, the Al_2O_3 surface coating on the cathode by other approaches usually increases the surface resistance of the cathode due to the low conductivity of Al_2O_3 [12–15] and leads to a lower specific capacity. We attribute the higher specific capacity of the modified NCM523 to the synergistic effect of the Al_2O_3 coating and the Al doping effect. The Al_2O_3 coating can mitigate the side reaction between the electrolyte and NCM523, which increases the conductivity of SEI. Additionally, doped Al can stabilize the surface lattice structure of NCM523, which can also promote Li diffusion into the surface of NCM523. This leads to less electrode overpotential and thus higher capacity under the same cut-off voltage [32–34]. This result is consistent with the

electrochemical test of the full cell using NCM523 with/without the surface modification. The specific capacity of NCM523 in the full cell increases from 178 to 187 mAh/g after the surface modification, as shown in Figure 4b.

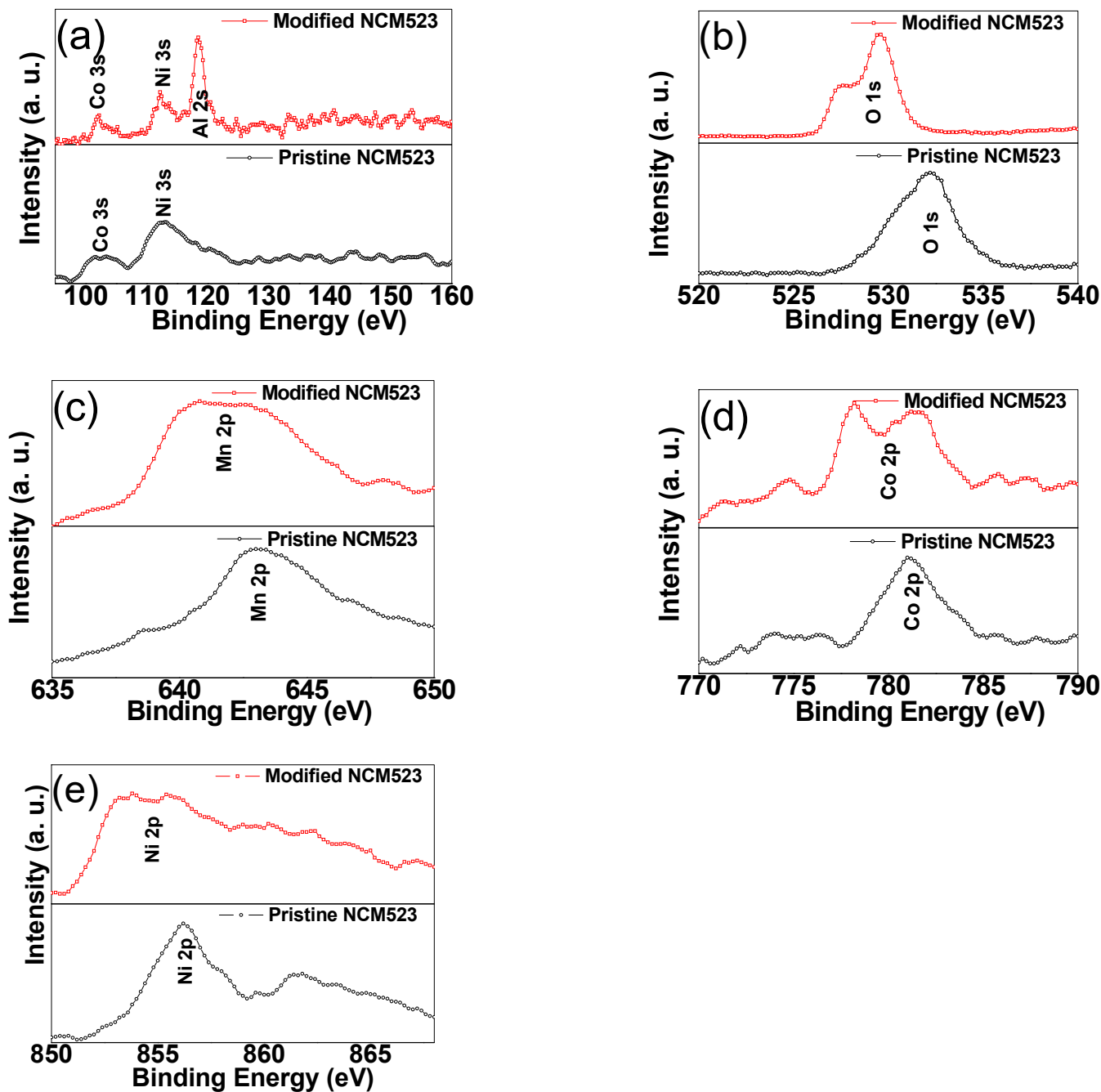


Figure 3. XPS (a) from 95 eV to 160 eV, (b) from 520 eV to 540 eV, (c) from 635 eV to 650 eV, (d) 770 eV to 790 eV and (e) from 850 eV to 870 eV of NCM523 with/without Al_2O_3 surface coating doping, suggesting that Al may not only exist as Al_2O_3 but that it also gets into the lattice structure of NCM523.

The beneficial effect of the Al-doped layer is supported by the rate performance of NCM523 in the half-cell (Figure 5a), which demonstrates that the increase in capacity for NCM523 after the surface modification is from 15% at C/10 to 21% at 2C. This is also consistent with the trend during rate tests of NCM523 in full cells seen in Figure 5c. Furthermore, the cycle test of NCM523 with a cut-off voltage of 4.5 V in half-cells demonstrated that

the capacity retention of NCM523 at C/3 can increase from 90% to 95% for 50 cycles. As shown in Figure 5b,d, the tendency of the results in the half-cells is consistent with those in the full cells. The ultra-thin $\text{Al}_2\text{O}_3/\text{NCMA}$ coating by this approach not only reduces the resistance of lithium diffusion through the surface, but also helps to maintain the stability of the resistance.

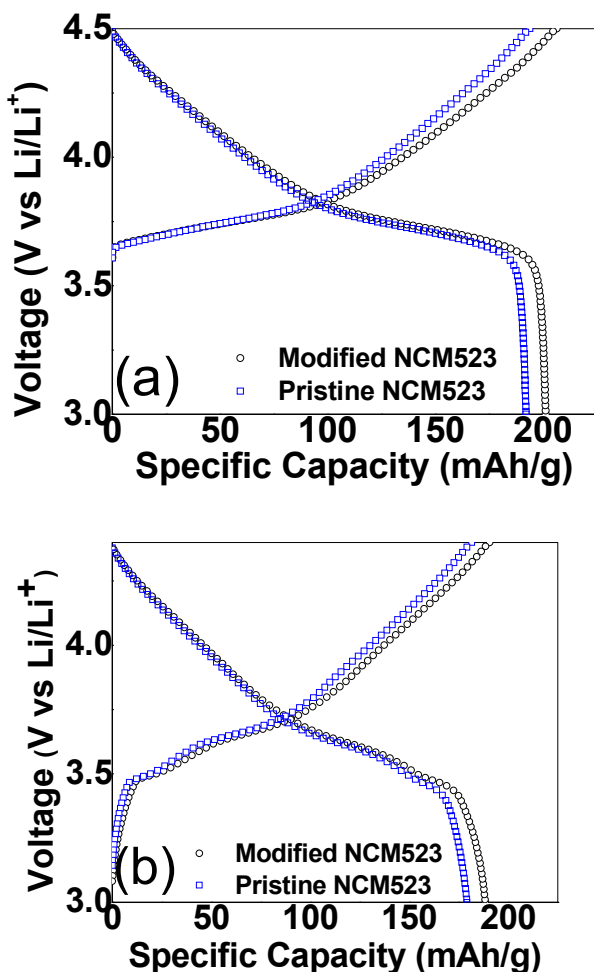


Figure 4. Voltage profile of NCM523 with/without coating doping in (a) half-cell and (b) full cell.

The ASI of pristine (Figure 6a) and modified (Figure 6b) NCM523 from the HPPC of half-cells during the cycle tests confirmed and further explored the effects of surface modification mentioned above. The ASI for pristine NCM523 is $41 \Omega \cdot \text{cm}^2$ at 50% DOD and $63 \Omega \cdot \text{cm}^2$ at 10% DOD during the first HPPC before the cycle tests. Meanwhile, the ASI of modified NCM523 is $36 \Omega \cdot \text{cm}^2$ at 50% DOD and $38 \Omega \cdot \text{cm}^2$ at 10% DOD. The impedance of the modified NCM523 is lower than that of the pristine one, especially much lower at 10% DOD, confirming the lower reaction resistance of modified NCM523. Furthermore, the ASI of the half-cell using pristine NCM523 increases by 120% from 41 to $90 \Omega \cdot \text{cm}^2$ at 50% DOD during the cycle test, while the ASI of the half-cell using modified NCM523 only increases by 50% from 24 to $36 \Omega \cdot \text{cm}^2$ at 50% DOD during the same cycle test. The impedance rise of the half-cell using modified NCM523 is much slower than that using pristine NCM523. This is the reason for which the capacity retention of the half-cell increases from 90% to 95% after replacing the pristine NCM523 with the modified NCM523. In addition, the ASI tendency of half-cells is consistent with that of full cells, where the ASI increases from 24 to $35 \Omega \cdot \text{cm}^2$ for the pristine NCM523 and 18 to $22 \Omega \cdot \text{cm}^2$ for the modified NCM523.

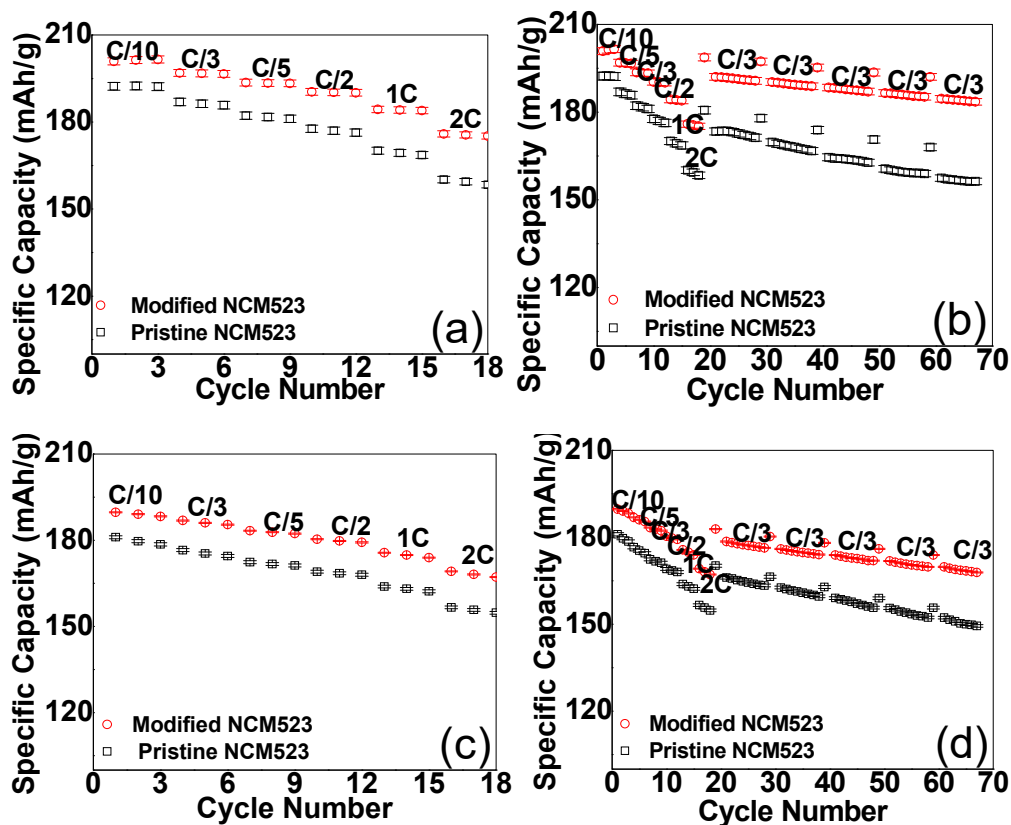


Figure 5. Rate (left) and cycling (right) tests of pristine NCM523 and NCM523 with Al_2O_3 coating doping in (a,b) half-cells and (c,d) full cells.

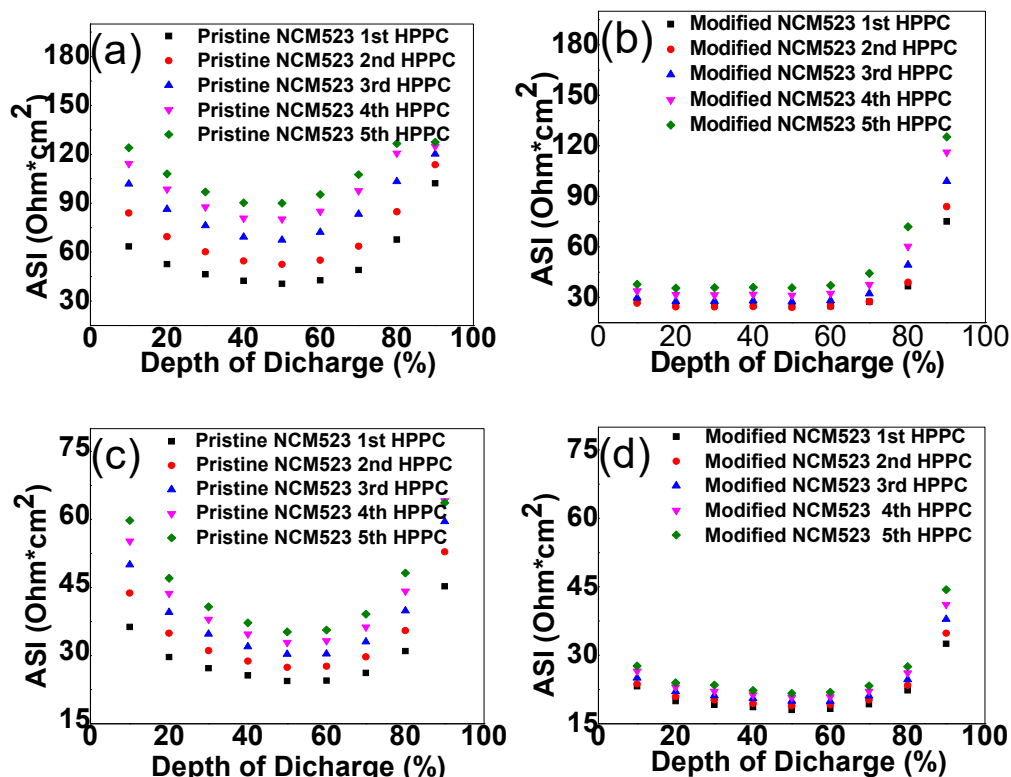


Figure 6. ASI of pristine NCM523 and NCM523 with Al_2O_3 coating doping in (a,b) half-cells and (c,d) full cells.

4. Conclusions

In summary, a new approach for the surface modification of NCM has been developed. This coating layer was found to have a strong interaction with the NCM and resulted in Al-doped NCM at the surface structure of NCM. The change of surface structure can not only reduce the surface resistance of lithium diffusion of NCM523, but also stabilize the solid electrolyte interface between NCM523 and the electrolyte with the cut-off voltage of 4.5 V vs. Li/Li⁺. The lower resistance and lower growth rate of resistance of NCM523 after modification increases its specific capacity (from 192 to 201 mAh/g) and capacity retention (90% to 95% for 50 cycles). Therefore, this scalable and effective method offers a valuable surface modification approach for academia and industry to further improve the performance of lithium-ion batteries to meet the growing demand.

Author Contributions: Conceptualization, X.W. and W.L.; formal analysis, X.S. and J.B.; investigation, X.S., X.W., J.B., Y.Q. and F.A.; resources, X.W.; data curation, X.S.; writing—original draft preparation, X.S.; writing—review and editing, W.L.; supervision, W.L.; project administration, W.L.; funding acquisition, X.S. and W.L. All authors have read and agreed to the published version of the manuscript.

Funding: This research was funded by DOE Office of Science laboratory under the contract of No. DE-AC02-06CH11357.

Acknowledgments: The support, which is from the U.S. Department of Energy’s (DOE) Office of Energy Efficiency & Renewable Energy (EERE) Vehicle Technologies Office, is gratefully acknowledged. Part of the work was carried out at the Electron Microscopy Center for Materials Research and the Center for Nanoscale Materials of Argonne National Laboratory (DOE Office of Science laboratory under the contract of No. DE-AC02-06CH11357). Xin Su also would like to thank the support of the Young Taishan Scholars Program of Shandong Province.

Conflicts of Interest: The authors declare no conflict of interest.

References

1. de Meatza, I.; Landa-Medrano, I.; Sananes-Israel, S.; Eguia-Barrio, A.; Bondarchuk, O.; Lijó-Pando, S.; Boyano, I.; Palomares, V.; Rojo, T.; Grande, H.-J.; et al. Influence of the Ambient Storage of LiNi_{0.8}Mn_{0.1}Co_{0.1}O₂ Powder and Electrodes on the Electrochemical Performance in Li-ion Technology. *Batteries* **2022**, *8*, 79. [[CrossRef](#)]
2. Coeler, M.; van Laack, V.; Langer, F.; Potthoff, A.; Höhn, S.; Reuber, S.; Koscheck, K.; Wolter, M. Infiltrated and Isostatic Laminated NCM and LTO Electrodes with Plastic Crystal Electrolyte Based on Succinonitrile for Lithium-Ion Solid State Batteries. *Batteries* **2021**, *7*, 11. [[CrossRef](#)]
3. Li, W.; Erickson, E.M.; Manthiram, A. High-nickel layered oxide cathodes for lithium-based automotive batteries. *Nat. Energy* **2020**, *5*, 26–34. [[CrossRef](#)]
4. Zappen, H.; Fuchs, G.; Gitis, A.; Sauer, D.U. In-Operando Impedance Spectroscopy and Ultrasonic Measurements during High-Temperature Abuse Experiments on Lithium-Ion Batteries. *Batteries* **2020**, *6*, 25. [[CrossRef](#)]
5. Singh, M.; Kaiser, J.; Hahn, H. Effect of Porosity on the Thick Electrodes for High Energy Density Lithium Ion Batteries for Stationary Applications. *Batteries* **2016**, *2*, 35. [[CrossRef](#)]
6. Baczyńska, A.; Niewiadomski, W.; Gonçalves, A.; Almeida, P.; Luís, R. Li-NMC Batteries Model Evaluation with Experimental Data for Electric Vehicle Application. *Batteries* **2018**, *4*, 11. [[CrossRef](#)]
7. Liu, Q.; Su, X.; Lei, D.; Qin, Y.; Wen, J.; Guo, F.; Wu, Y.A.; Rong, Y.; Kou, R.; Xiao, X.; et al. Approaching the capacity limit of lithium cobalt oxide in lithium ion batteries via lanthanum and aluminium doping. *Nat. Energy* **2018**, *3*, 936–943. [[CrossRef](#)]
8. Kosova, N.; Devyatkina, E.; Kaichev, V. Optimization of Ni²⁺/Ni³⁺ ratio in layered Li(Ni,Mn,Co)O₂ cathodes for better electrochemistry. *J. Power Sources* **2007**, *174*, 965–969. [[CrossRef](#)]
9. Cherkashinin, G.; Motzko, M.; Schulz, N.; Späth, T.; Jaegermann, W. Electron Spectroscopy Study of Li[Ni,Co,Mn]O₂/Electrolyte Interface: Electronic Structure, Interface Composition, and Device Implications. *Chem. Mater.* **2015**, *27*, 2875–2887.
10. Xiong, C.; Liu, F.; Gao, J.; Jiang, X. One-Spot Facile Synthesis of Single-Crystal LiNi_{0.5}Co_{0.2}Mn_{0.3}O₂ Cathode Materials for Li-ion Batteries. *ACS Omega* **2020**, *5*, 30356–30362. [[CrossRef](#)]
11. Klein, S.; Bärmann, P.; Beuse, T.; Borzutzki, K.; Frerichs, J.E.; Kasnatscheew, J.; Winter, M.; Placke, T. Exploiting the Degradation Mechanism of NCM523 Graphite Lithium-Ion Full Cells Operated at High Voltage. *ChemSusChem* **2021**, *14*, 595–613. [[CrossRef](#)]
12. Cao, G.; Jin, Z.; Zhu, J.; Li, Y.; Xu, B.; Xiong, Y.; Yang, J. A green Al₂O₃ metal oxide coating method for LiNi_{0.5}Co_{0.2}Mn_{0.3}O₂ cathode material to improve the high voltage performance. *J. Alloys Compd.* **2020**, *832*, 153788. [[CrossRef](#)]
13. Neudeck, S.; Mazilkin, A.; Reitz, C.; Hartmann, P.; Janek, J.; Brezesinski, T. Effect of Low-Temperature Al₂O₃ ALD Coating on Ni-Rich Layered Oxide Composite Cathode on the Long-Term Cycling Performance of Lithium-Ion Batteries. *Sci. Rep.* **2019**, *9*, 5328. [[CrossRef](#)]

14. Shi, Y.; Zhang, M.; Qian, D.; Meng, Y.S. Ultrathin Al_2O_3 Coatings for Improved Cycling Performance and Thermal Stability of $\text{LiNi}_{0.5}\text{Co}_{0.2}\text{Mn}_{0.3}\text{O}_2$ Cathode Material. *Electrochim. Acta* **2016**, *203*, 154–161. [CrossRef]
15. Zhao, L.; Chen, G.; Weng, Y.; Yan, T.; Shi, L.; An, Z.; Zhang, D. Precise Al_2O_3 Coating on $\text{LiNi}_{0.5}\text{Co}_{0.2}\text{Mn}_{0.3}\text{O}_2$ by Atomic Layer Deposition Restrains the Shuttle Effect of Transition Metals in Li-Ion Capacitors. *Chem. Eng. J.* **2020**, *401*, 126138. [CrossRef]
16. Guan, P.; Zhou, L.; Yu, Z.; Sun, Y.; Liu, Y.; Wu, F.; Jiang, Y.; Chu, D. Recent progress of surface coating on cathode materials for high-performance lithium-ion batteries. *J. Energy Chem.* **2020**, *43*, 220–235. [CrossRef]
17. Hou, Q.; Cao, G.; Wang, P.; Zhao, D.; Cui, X.; Li, S.; Li, C. Carbon coating nanostructured- $\text{LiNi}_{1/3}\text{Co}_{1/3}\text{Mn}_{1/3}\text{O}_2$ cathode material synthesized by chemical vapor deposition method for high performance lithium-ion batteries. *J. Alloys Compd.* **2018**, *747*, 796–802. [CrossRef]
18. Son, H.I.; Park, K.; Park, J.H. Improvement in high-voltage and high rate cycling performance of nickel-rich layered cathode materials via facile chemical vapor deposition with methane. *Electrochim. Acta* **2017**, *230*, 308–315.
19. Qiu, B.; Wang, J.; Xia, Y.; Wei, Z.; Han, S.; Liu, Z. Enhanced Electrochemical Performance with Surface Coating by Reactive Magnetron Sputtering on Lithium-Rich Layered Oxide Electrodes. *ACS Appl. Mater. Interfaces* **2014**, *6*, 9185–9193. [CrossRef]
20. Yu, H.; Wang, S.; Hu, Y.; He, G.; Bao, L.Q.; Parkin, I.P.; Jiang, H. Lithium-conductive LiNbO_3 coated high-voltage $\text{LiNi}_{0.5}\text{Co}_{0.2}\text{Mn}_{0.3}\text{O}_2$ cathode with enhanced rate and cyclability. *Green Energy Environ.* **2020**, *7*, 266–274. [CrossRef]
21. Yao, C.; Mo, Y.; Jia, X.; Chen, X.; Xia, J.; Chen, Y. LiMnPO_4 surface coating on $\text{LiNi}_{0.5}\text{Co}_{0.2}\text{Mn}_{0.3}\text{O}_2$ by a simple sol-gel method and improving electrochemical properties. *Solid State Ion.* **2018**, *317*, 156–163. [CrossRef]
22. Zhou, H.; Yu, S.; Liu, H.; Liu, P. Protective coatings for lithium metal anodes: Recent progress and future perspectives. *J. Power Sources* **2020**, *450*, 227632. [CrossRef]
23. Xu, Q.; Li, X.; Kheimeh Sari, H.M.; Li, W.; Liu, W.; Hao, Y.; Qin, J.; Cao, B.; Xiao, W.; Xu, Y.; et al. Surface engineering of $\text{LiNi}_{0.8}\text{Mn}_{0.1}\text{Co}_{0.1}\text{O}_2$ towards boosting lithium storage: Bimetallic oxides versus monometallic oxides. *Nano Energy* **2020**, *77*, 105034. [CrossRef]
24. Ahn, J.; Jang, E.K.; Yoon, S.; Lee, S.-J.; Sung, S.-J.; Kim, D.-H.; Cho, K.Y. Ultrathin ZrO_2 on $\text{LiNi}_{0.5}\text{Mn}_{0.3}\text{Co}_{0.2}\text{O}_2$ electrode surface via atomic layer deposition for high-voltage operation in lithium-ion batteries. *Appl. Surf. Sci.* **2019**, *484*, 701–709. [CrossRef]
25. Su, L.; Weaver, J.L.; Groenenboom, M.; Nakamura, N.; Rus, E.; Anand, P.; Jha, S.K.; Okasinski, J.S.; Dura, J.A.; Reeja-Jayan, B. Tailoring Electrode-Electrolyte Interfaces in Lithium-Ion Batteries Using Molecularly Engineered Functional Polymers. *ACS Appl. Mater. Interfaces* **2021**, *13*, 9919–9931. [CrossRef]
26. Xu, G.-L.; Liu, Q.; Lau, K.K.S.; Liu, Y.; Liu, X.; Gao, H.; Zhou, X.; Zhuang, M.; Ren, Y.; Li, J.; et al. Building ultraconformal protective layers on both secondary and primary particles of layered lithium transition metal oxide cathodes. *Nat. Energy* **2019**, *4*, 484–494. [CrossRef]
27. Su, L.; Smith, P.M.; Anand, P.; Reeja-Jayan, B. Surface Engineering of a LiMn_2O_4 Electrode Using Nanoscale Polymer Thin Films via Chemical Vapor Deposition Polymerization. *ACS Appl. Mater. Interfaces* **2018**, *10*, 27063–27073. [CrossRef]
28. Zhang, Y.; Kim, C.S.; Song, H.W.; Chang, S.-J.; Kim, H.; Park, J.; Hu, S.; Zhao, K.; Lee, S. Ultrahigh active material content and highly stable Ni-rich cathode leveraged by oxidative chemical vapor deposition. *Energy Storage Mater.* **2022**, *48*, 1–11. [CrossRef]
29. Tago, T.; Kataoka, N.; Tanaka, H.; Kinoshita, K.; Kishida, S. XPS study from a clean surface of Al_2O_3 single crystals. *Procedia Eng.* **2017**, *216*, 175–181. [CrossRef]
30. Singh, A.N.; Kim, M.-H.; Meena, A.; Wi, T.-U.; Lee, H.-W.; Kim, K.S. Na/Al Codoped Layered Cathode with Defects as Bifunctional Electrocatalyst for High-Performance Li-Ion Battery and Oxygen Evolution Reaction. *Small* **2021**, *17*, 2005605. [CrossRef]
31. Oh, J.; Kim, J.; Lee, Y.M.; Shin, D.O.; Kim, J.Y.; Lee, Y.-G.; Kim, K.M. High-rate cycling performance and surface analysis of $\text{LiNi}_{1-x}\text{Co}_x/2\text{Mn}_{x/2}\text{O}_2$ ($x = 2/3, 0.4, 0.2$) cathode materials. *Mater. Chem. Phys.* **2019**, *222*, 1–10. [CrossRef]
32. Kim, U.-H.; Kuo, L.-Y.; Kaghazchi, P.; Yoon, C.; Sun, Y. Quaternary Layered Ni-Rich NCMA Cathode for Lithium-Ion Batteries. *ACS Energy Lett.* **2019**, *4*, 576–582. [CrossRef]
33. Song, X.; Liu, G.; Yue, H.; Luo, L.; Yang, S.; Huang, Y.; Wang, C. A novel low-cobalt long-life $\text{LiNi}_{0.88}\text{Co}_{0.06}\text{Mn}_{0.03}\text{Al}_{0.03}\text{O}_2$ cathode material for lithium ion batteries. *Chem. Eng. J.* **2021**, *407*, 126301. [CrossRef]
34. Fly, A.; Chen, R. Rate dependency of incremental capacity analysis (dQ/dV) as a diagnostic tool for lithium-ion batteries. *J. Energy Storage* **2020**, *29*, 101329. [CrossRef]